Electronic Supplementary Material (ESI) for Materials Chemistry Frontiers.


# Supporting Information

## Visible light, Temperature, and Electric Field-Driven Rotation of Diffraction Gratings Enabled by a Novel Axially Chiral Molecular Switch

Xinfang Zhang,‡[a] Fathy Hassan,‡[ab] Hari Krishna Bisoyi,[a] Hao Wang,[a] Ziyuan Zhou,[a] and Quan Li*[ac]

[a]Advanced Materials and Liquid Crystal Institute and Materials Science Graduate Program, Kent State University, Kent, Ohio 44242, USA

[b]Department of Chemistry, Faculty of Science, Tanta University, Tanta, El-Gharbia 31527, Egypt

[c]Institute of Advanced Materials and School of Chemistry and Chemical Engineering Southeast University, Nanjing, Jiangsu 211189, China

*: E-mail: quanli3273@gmail.com

‡: X. Zhang and F. Hassan contributed equally to this work.

# Table of Contents



## 1. Experimental

### 1.1. Materials and methods

Unless otherwise noted, chemicals and solvents were purchased from commercial suppliers and were used as received without further purification. (*R*)-1,1′-Binaphthyl-2,2′-diamine ((*R*)-BINAM), 4-bromoaniline, tetrakis(triphenylphosphine) palladium(0) ($Pd(PPh_3)_4$), potassium peroxymonosulfate (OXONE), potassium carbonate ($K_2CO_3$), magnesium sulfate ($MgSO_4$), acetic acid, anhydrous tetrahydrofuran (THF), dichloromethane (DCM), deuterated chloroform ($CDCl_3$), deuterated 1,4-dioxane ($C_4D_8O_2$), and 1,4-dioxane (spectroscopic grade) were purchased from Sigma-Aldrich. (4-n-Pentylphenyl)boronic acid was purchased from Tokyo Chemical Industry Co., Ltd. Achiral nematic liquid crystal E7 was used as the host in the study (Merck, $\Delta\varepsilon$ = 13.8 at f = 1 kHz, $\Delta n$ = 0.223 at 25 ℃, $K_{11}$ = 11.7 pN, $K_{22}$ = 6.8 pN and $K_{33}$ = 17.8 pN, $T_{N\text{-}I}$ = 59.8 ℃) and were purchased from Jiangsu Hecheng Display Technology Co., Ltd.

$^1$H- and $^{13}$C-NMR spectra were recorded on a Bruker 400 MHz NMR spectrometer using $CDCl_3$ as a solvent. Chemical shifts are in $\delta$ unit (ppm) with the residual solvent peak as the internal standard. The coupling constant (*J*) is reported in hertz (Hz). NMR splitting patterns are designed as follows: s, singlet; d, doublet; t, triplet; q: quartet, and m, multiplet. High-resolution mass spectra (HRMS) were obtained using an Exactive Plus mass spectrometer (Thermo Scientific, Bremen, Germany). Isotopic patterns were simulated using the software Thermo Xcalibur 3.0.63 (Thermo Scientific, Bremen, Germany). Column chromatography was carried out on silica gel (230-400 mesh). Analytical thin layer chromatography (TLC) was performed on commercially aluminum backed silica gel (200 micron). Spots on the TLC plates were visualized by exposing to UV light.

Polarized optical microscopy (POM) (transmission mode) with a Leitz polarizing microscope was used to see the mixing boundary from miscibility test, the rotational behavior of the cholesteric liquid crystal (CLC) gratings by triple external stimuli, and disclination lines from the traditional Grandjean-Cano wedge cell. POM (Nikon, Optiphot2-POL) in reflection mode was used to observe CLC varying with electric fields in a planar cell. The visible light (405 nm, 1.5 mW/cm$^2$ and 520 nm, 2.2 mW/cm$^2$) irradiation were obtained from Xenon light source (100 W) filtered through 405 nm and 520 nm filters.

A hot stage (FP90, Mettler) was used to increase the temperature of CLC system, resulting in pitch increased and phase transition from cholesteric phase to isotropic phase. Alternating current (AC, 1 kHz) was applied via a function generator. UV-Vis absorption spectra were

recorded by a Perkin Elmer Lambda 25 Spectrometer. Circular dichroism (CD) spectra were obtained using Aviv 410 CD spectrophotometer. Reflection spectra were measured with an Ocean Optics USB2000+ spectrometer in the dark. A red laser diode (633 nm, 1 mW) and the unpolarized collimated white-light with a pinhole or a rectangular slit (width: 0.25 mm and height: 1.3 mm), perpendicular to both the planar cell and the projection screen/camera, were used. The diffraction patterns can be seen separately in the digital camera (Canon) and in the CCD camera.

The commercially available planar cells (INSTEC, cell gap = 5.0 μm) with antiparallel rubbing directions of polyimide alignment layers on both indium-tin-oxide (ITO)-covered glass substrates were used to explore the *trans-cis* photoisomerization behavior in high concentration mixture. The CLC mixture was filled into the planar cell by capillary force at room temperature. To observe the selective reflection color more clearly, the back side of the planar cell was painted with black paint. The hybrid cell based on both indium-tin-oxide (ITO)-covered glass substrates possesses one planar alignment layer and another vertical alignment layer, leading to a spontaneously periodic distortion and striped domains oriented unidirectionally. The cell gap is 5.0 μm and the area of transparent electrode is $1 \times 1$ cm$^2$. The CLC mixtures with different concentrations were filled into cells by capillary forces at room temperature.

### 1.2. Synthesis and characterization of visible light-driven axially chiral molecular switch (*R*)-1

The synthetic pathway of the axially chiral molecular switch (*R*)-**1** is shown in **Scheme S1**. First, 1-bromo-4-nitrosobenzene (**NOPhBr**) was synthesized by OXONE oxidation of 4-bromoaniline in a biphasic system. Then, the obtained nitroso species was reacted with (*R*)-BINAM in presence of acetic acid to yield the intermediate (**DiBrAzo**). By a palladium catalyzed Suzuki-Miyaura reaction, the obtained **DiBrAzo** was reacted with (4-n-pentylphenyl)boronic acid to yield (*R*)-**1**. The experimental details of each step as follows:

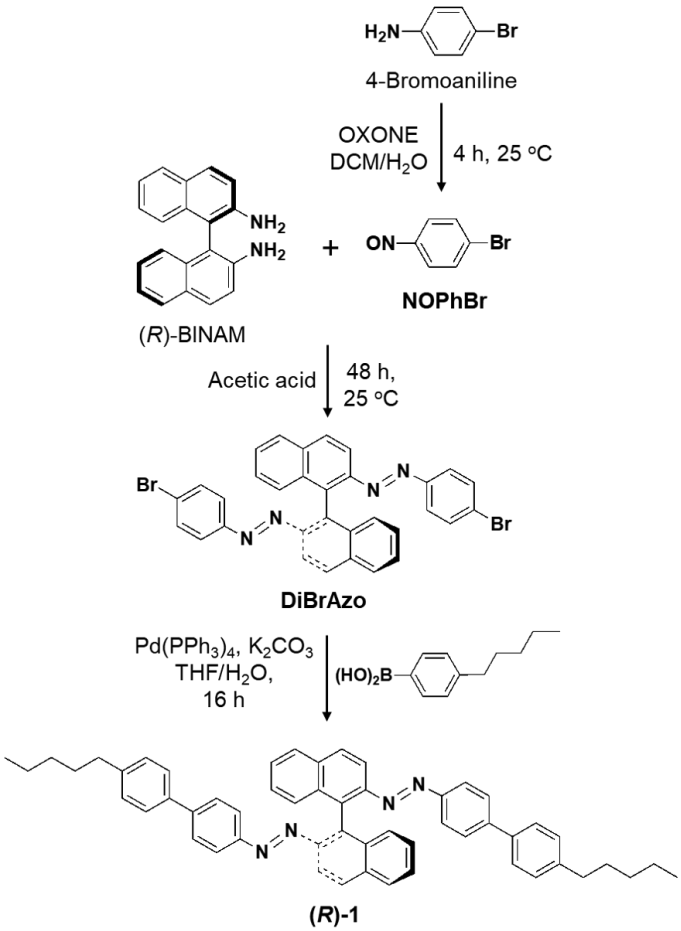


**Scheme S1.** Synthesis of the axially chiral molecular switch (*R*)-**1**.

**NOPhBr**.[S1] 4-Bromoaniline (3 g, 17.8 mmol) was dissolved in DCM (75 mL). To this solution, OXONE (21.5 g, 35.7 mmol) dissolved in water (150 mL) was added. The solution mixture was stirred under argon at room temperature until TLC monitoring indicated complete consumption of the starting material (3 h). After separation of the layers, the aqueous layer was extracted with DCM twice. The combined organic layers were washed with 1N HCl, saturated sodium bicarbonate solution, water, brine and dried over $MgSO_4$. Removal of the solvent was carried out under reduced pressure at room temperature. The crude product was purified directly by column chromatography on silica gel yielded 2.35 g (55%) of **NOPhBr** as a green solid which was stored at -5 ℃. $^1$H NMR ($CDCl_3$, 400 MHz, **Figure S13 (a)**): $\delta$ = 7.77 (s, 4H, Ar H). $^{13}$C NMR ($CDCl_3$, 400 MHz, **Figure S13 (b)**): $\delta$ = 122.12 ($C_2$), 131.70 ($C_4$), 132.71 ($C_3$), 163.83 ($C_1$) ppm.

**DiBrAzo.** (*R*)-BINAM (0.3 g, 1.05 mmol) was dissolved in acetic acid (30 mL). To this solution, compound **1** (0.42 g, 2.3 mmol) dissolved in acetic acid (30 mL) was added. The reaction mixture was stirred for 48 h at 25 ℃ under argon. The resulting mixture was quenched by

distilled water (200 mL), extracted with DCM (300 mL), and dried over $MgSO_4$. The solvent was evaporated under reduced pressure, and the residue was purified by column chromatography on silica gel to afford **DiBrAzo** (0.34 g, 52%) as a red powder. $^1$H NMR ($CDCl_3$, 400 MHz, **Figure S14 (a)**): $\delta$ = 7.18–7.20 (d, 4H, *J* = 8.8 Hz), 7.30–7.38 (m, 6H), 7.49–7.57 (m, 4H), 8.00–8.02 (d, 2H, *J* = 8 Hz), 8.08–8.10 (d, 2H, *J* = 8.6 Hz), 8.17–8.19 (d, 2H, *J* = 8 Hz). $^{13}$C NMR ($CDCl_3$, 400 MHz, **Figure S14 (b)**): $\delta$ = 114.11, 124.18, 124.95, 126.89, 127.57, 127.91, 128.20, 129.34, 132.02, 134.14, 134.59, 137.65, 148.18, 151.48 ppm. HRMS calcd. for $C_{32}H_{20}Br_2N_4$ ($[M+H]^+$): 621.0107, found: 621.0106.

**(*R*)-1**. To a solution of compound **DiBrAzo** (0.2 g, 0.3 mmol) in anhydrous THF (50 mL), (4-n-pentylphenyl)boronic acid (0.13 g, 0.66 mmol) was added under argon. To this mixture, a solution of $K_2CO_3$ (0.18 g, 1.32 mmol) in distilled water (15 mL) was added. After stirring under reduced pressure, $Pd(PPh_3)_4$ (35 mg, 0.03 mmol) catalyst was added. The reaction mixture was refluxed for 16 h at 80 ℃ under argon. TLC analysis showed completion of the reaction. THF was removed under vacuum. The residue was extracted with DCM (300 mL) and water (200 mL). The organic layer was dried over $MgSO_4$ and concentrated under reduced pressure. It was then purified by column chromatography over silica gel to afford (*R*)-**1** (0.13 g, 53%) as a red powder. $^1$H NMR ($CDCl_3$, 400 MHz, **Figure S15 (a)**): $\delta$ = 0.90–0.94 (t, 6H, J = 8 Hz), 1.29–1.36 (m, 8H), 1.63–1.69 (m, 4H), 2.62–2.66 (t, 4H, *J* = 8.8 Hz), 7.20–7.22 (d, 2H, *J* = 8 Hz), 7.29–7.23 (d, 2H, *J* = 8.8 Hz), 7.39–7.55 (m, 16H), 8.01–8.03 (d, 2H, *J* = 8 Hz), 8.09–8.11 (d, 2H, *J* = 8 Hz), 8.22–8.24 (d, 2H, *J* = 8.8 Hz). $^{13}$C NMR ($CDCl_3$, 400 MHz, **Figure S15 (b)**): $\delta$ = 14.05, 22.57, 31.12, 31.55, 35.60, 114.38, 123.29, 126.74, 126.88, 127.25, 127.94, 128.14, 128.86, 129.16, 134.31, 134.51, 137.44, 137.48, 142.70, 143.17, 148.48, 151.85 ppm. HRMS calcd. for $C_{54}H_{50}N_4$ ($[M+H]^+$): 755.4108, found: 755.4107.

## 2. Results and Discussion

### 2.1. *trans*:*cis* ratio in the photostationary state of (*R*)-1

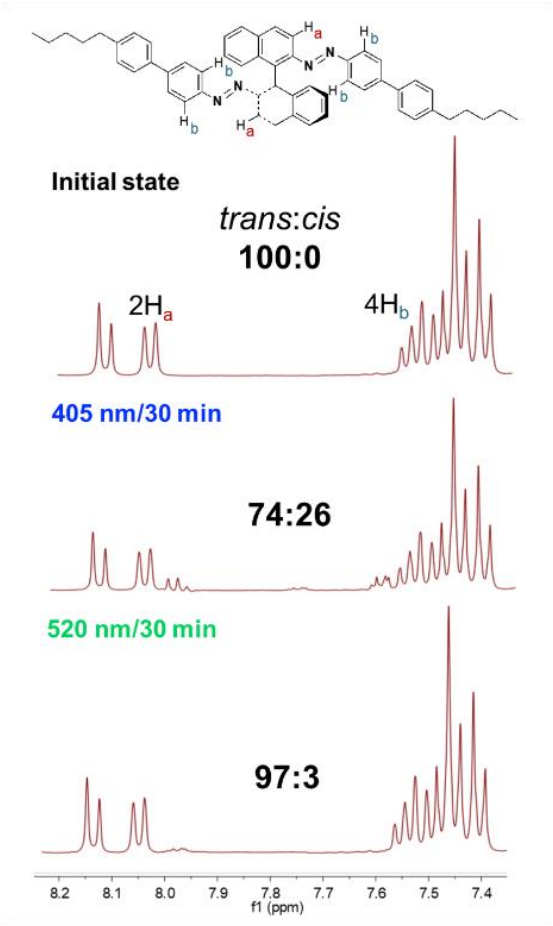


**Figure S1**. $^{1}$H-NMR spectra of the hydrogen atoms close to the azo group of (*R*)-**1** in deuterated 1,4-dioxane. *trans*:*cis* ratio was determined from the area under peaks upon visible light irradiation by 405 nm (1.5 mW cm$^{-2}$) for 30 min followed by 520 nm (2.2 mW cm$^{-2}$) light irradiation for 30 min in sequence.

## 2.2. Handedness validation of CLC mixture

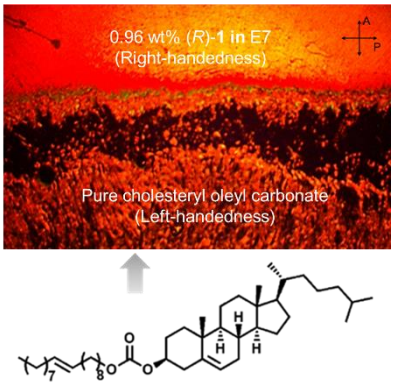


**Figure S2.** POM image from the miscibility test performed between the sample mixture (0.96 wt% (*R*)-**1** in E7) and pure cholesteryl oleyl carbonate (left-handed).

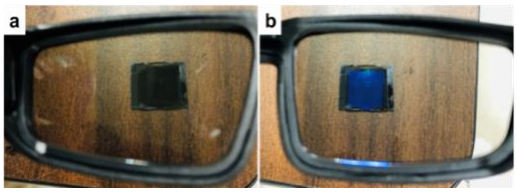


**Figure S3.** Blue selective reflection in a planar cell observed by the 3D goggle: (a) no transmission (left glass) and (b) transmission (right glass), indicating that CLC sample has right-handedness.

### 2.3. Photochemically and thermally driven RGB colors

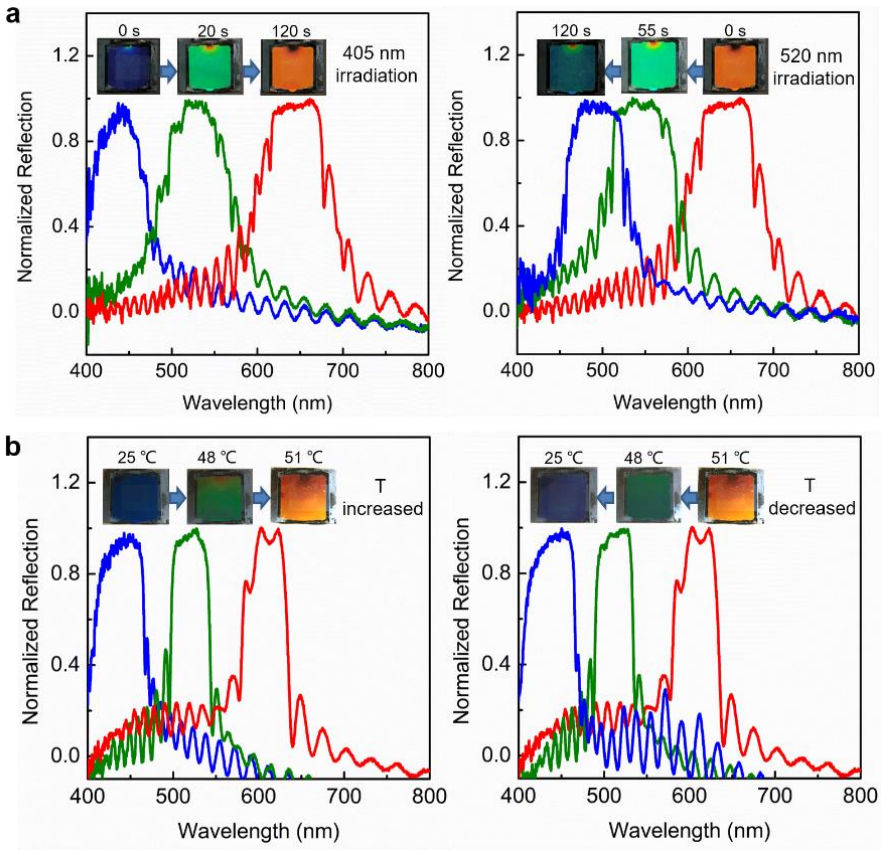


**Figure S4.** (a) Visible light-driven (405 nm, 1.5 mW $cm^{-2}$ and 520 nm, 2.2 mW $cm^{-2}$) and (b) temperature-driven reflection spectra in a 5 μm planar cell (painted black on the back side) filled with 3.4 wt% molecular switch (*R*)-**1** in E7. The insert real cell photos are corresponding to each reflection curve.

### 2.4. POM images of CLC under the effect of electric fields in a planar cell

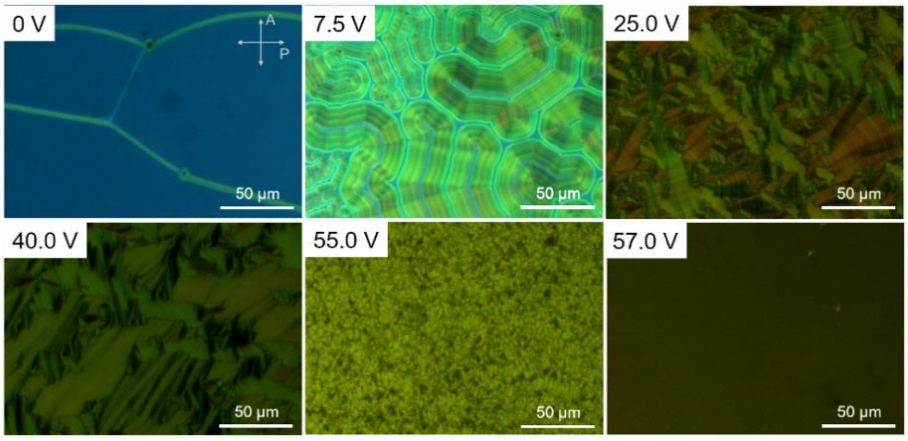


**Figure S5.** POM images (reflection mode) of CLC with varying electric fields in a 5 μm planar cell (painted black on the back side) filled with 3.4 wt% of (*R*)-**1** in E7.

### 2.5. CLC gratings in hybrid-aligned cells

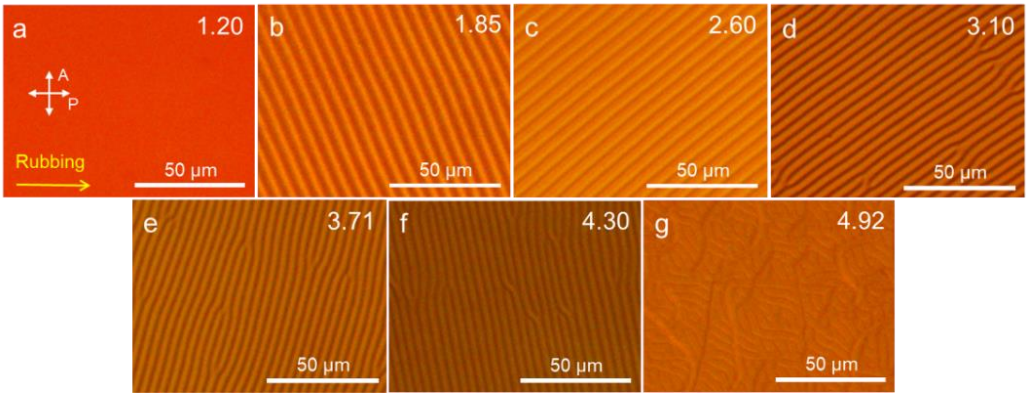


**Figure S6.** POM images of CLC mixture with different concentrations of chiral dopant in hybrid cells with same cell thickness (5 μm) without any external stimuli (a) d/*P*=1.20, (b) d/*P*=1.85, (c) d/*P*=2.60, (d) d/*P*=3.10, (e) d/*P*=3.71, (f) d/*P*=4.30, (g) d/*P*=4.92.

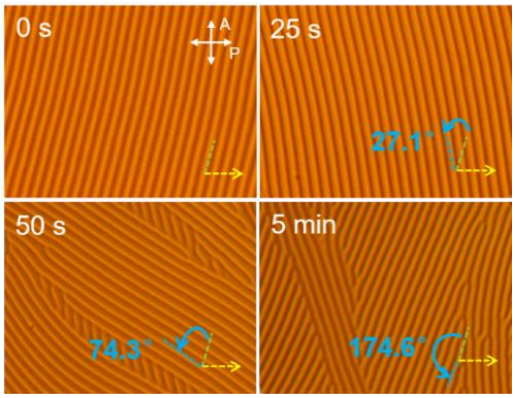


**Figure S7.** POM images of the counterclockwise rotation process of the CLC grating by 520 nm visible light (2.2 mW $cm^{-2}$) irradiation based on 405 nm irradiation 3 min at the initial d/*P* ratio of 4.30. (The yellow arrow represents the rubbing direction of the planar alignment layer, and the green dotted line and the blue dotted line represent the initial and the final stripe direction of CLC grating, respectively).

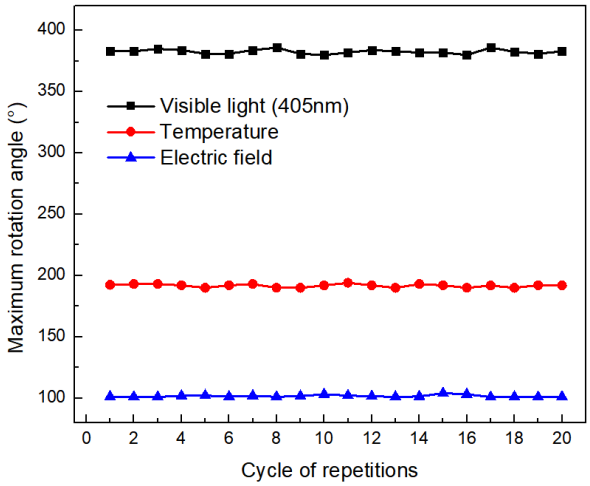


**Figure S8.** Fatigue resistance measurement of CLC grating under the three different external stimuli respectively: visible light (405 nm and initial d/*P* ratio is 4.30), temperature (initial d/*P* ratio is 4.30), and electric field (initial d/*P* ratio is 1.85).

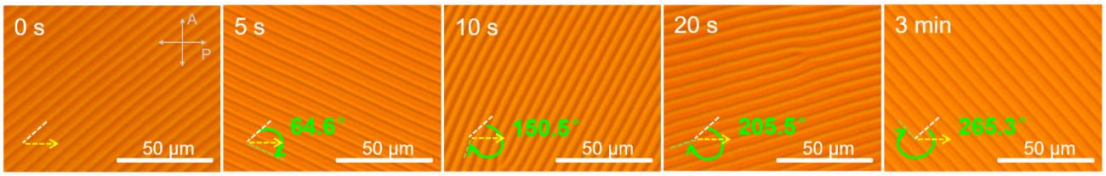


**Figure S9.** POM images of the clockwise rotation process of the CLC grating by 405 nm visible light (1.5 mW $cm^{-2}$) irradiation at the initial d/*P* ratio of 2.60. (The yellow arrow represents the rubbing direction of the planar alignment layer, the white dotted line and the green dotted line represent the initial and the final stripe direction of CLC grating, respectively).

## 2.6. Diffraction experiment

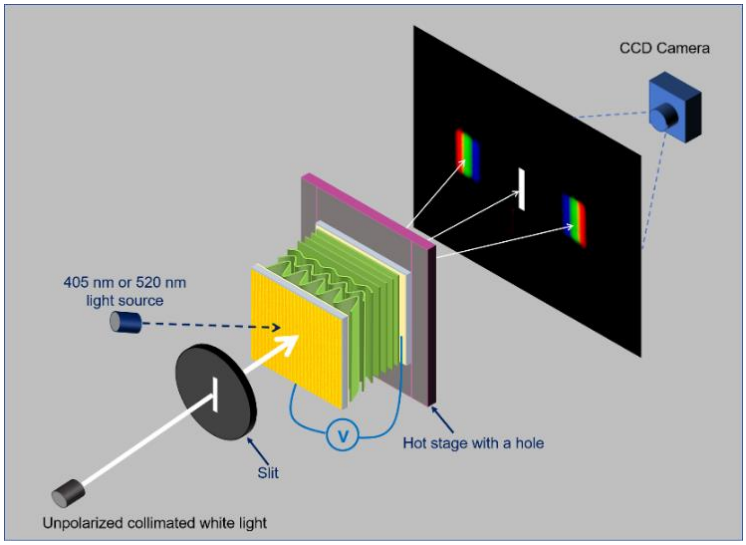


**Figure S10.** Schematic illustration of diffraction experimental set-up with the unpolarized collimated white-light as probing beam passing through a rectangular slit.

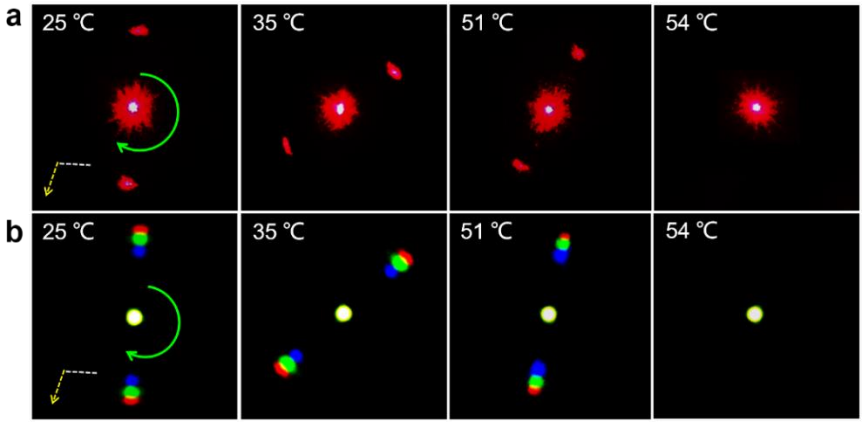


**Figure S11.** Diffraction patterns with (a) the red laser diode (633 nm, 1 mW) and (b) the unpolarized collimated white light with a pinhole as probing beams resulting from the in-plane rotation of CLC grating (initial d/*P*=4.30) driven by temperature. (The yellow arrow represents the rubbing direction of the planar alignment layer, and the white dotted line represents the initial stripe direction of CLC grating).

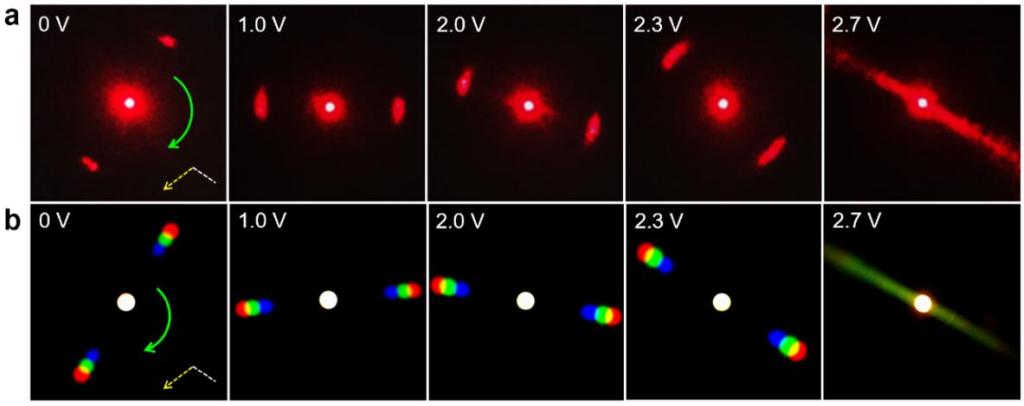


**Figure S12.** Diffraction patterns with (a) the red laser diode (633 nm, 1 mW) and (b) the unpolarized collimated white light with a pinhole as probing beams resulting from the in-plane rotation of CLC grating (initial d/*P*=1.85) driven by electric fields. (The yellow arrow represents the rubbing direction of the planar alignment layer, and the white dotted line represents the initial stripe direction of CLC grating).

## 3. $^{1}$H- and $^{13}$C-NMR spectra

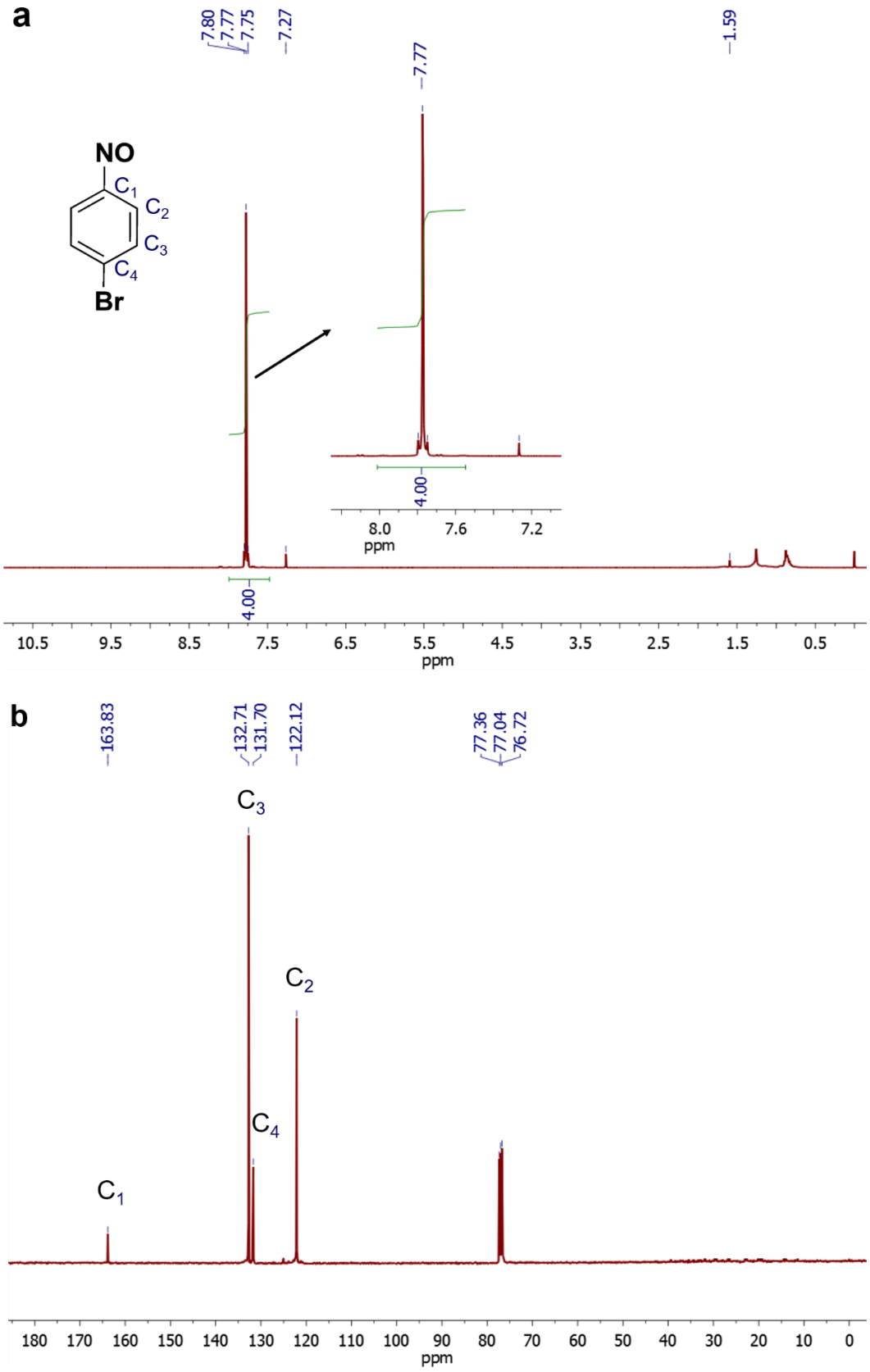


**Figure S13.** $^{1}$H-NMR (a) and $^{13}$C-NMR (b) spectra of **NOPhBr** in $CDCl_3$.

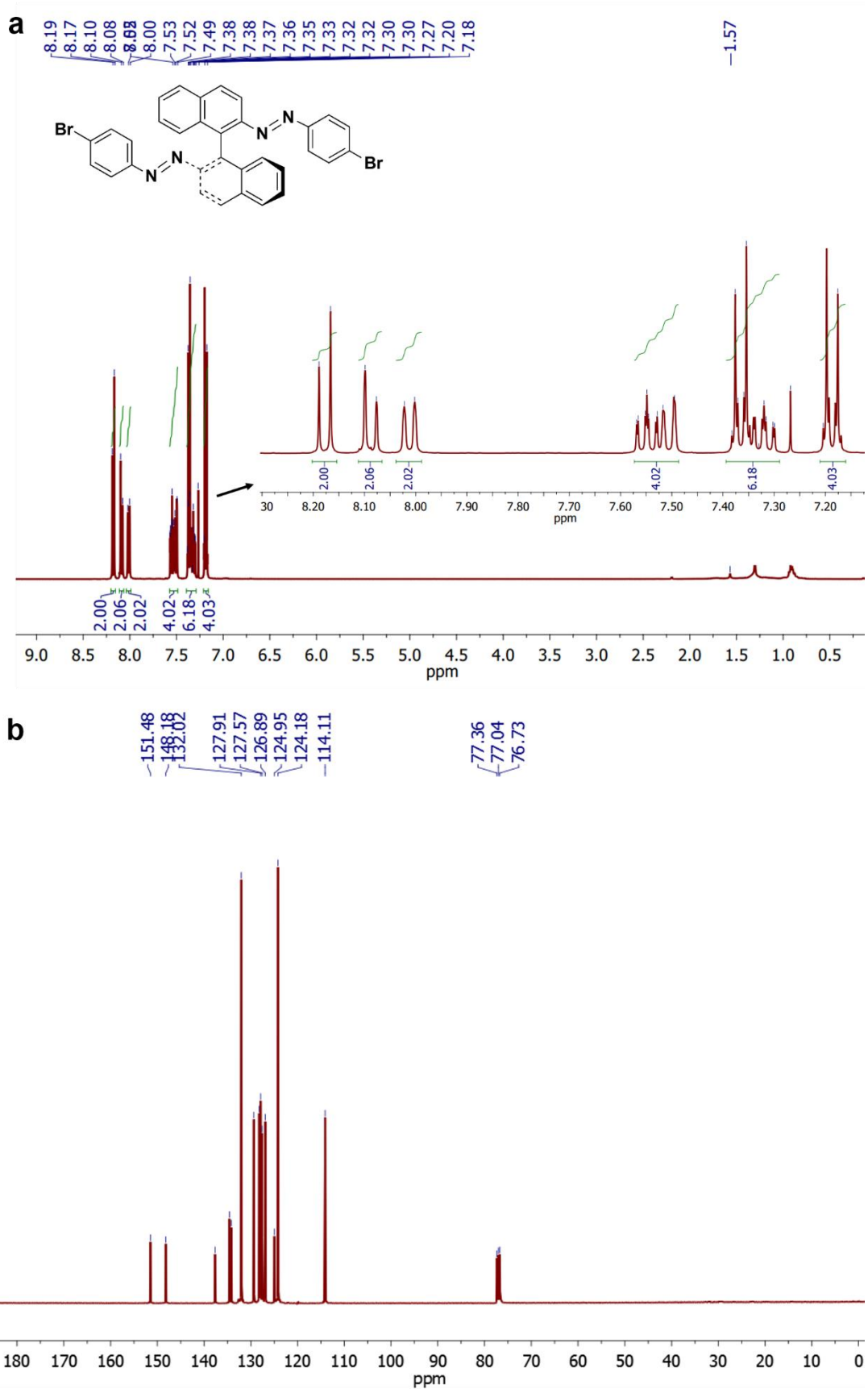


**Figure S14.** $^{1}$H-NMR (a) and $^{13}$C-NMR (b) spectra of **DiBrAzo** in $CDCl_3$.

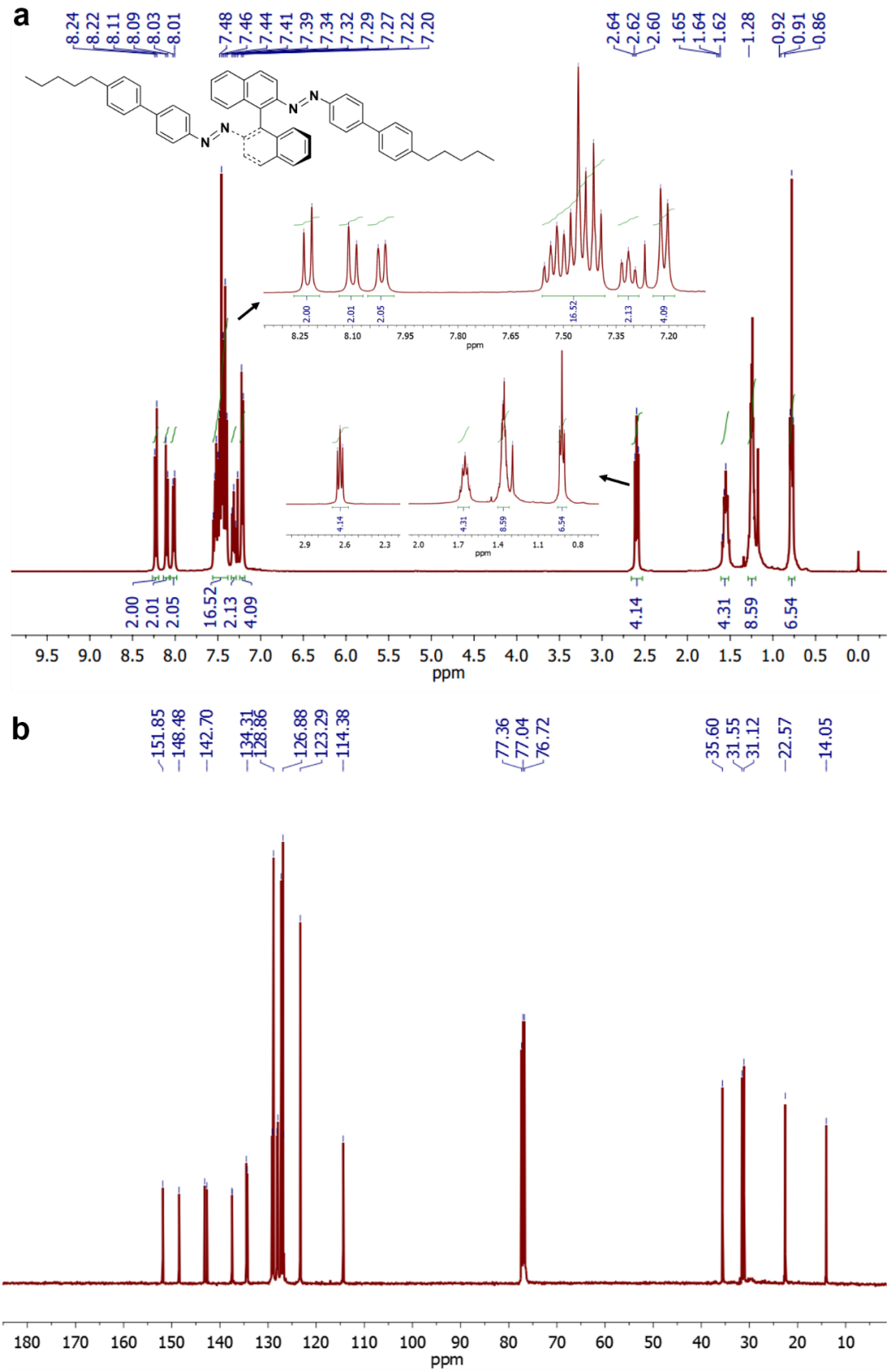


**Figure S15.** $^{1}$H-NMR (a) and $^{13}$C-NMR (b) spectra of (*R*)-**1** in $CDCl_3$.

## 4. References

S1 B. Priewisch and K. Braun, Efficient preparation of nitrosoarenes for the synthesis of azobenzenes, *J. Org. Chem.* 2005, **70**, 2350-2352.